Heterogeneity and Probabilistic Binding Contributions to Receptor-mediated Cell Detachment Kinetics

Ann Saterbak, Suzanne C. Kuo, and Douglas A. Lauffenburger
Department of Chemical Engineering, University of Illinois at Urbana-Champaign, Urbana, Illinois 61801 USA

ABSTRACT Biospecific cell adhesion is mediated by receptor-ligand bonds. Early theoretical work presented a deterministic analysis of receptor-mediated cell attachment and detachment for a homogenous cell population. However, initial comparison of a deterministic framework to experimental detachment profiles of model "cells" (antibody-coated latex beads) did not show qualitative or quantitative agreement (Cozens-Roberts, C., D. A. Lauffenburger, and J. A. Quinn. 1990. *Biophys. J.* 58:857–872). Hence, we determine the contributions of population heterogeneity and probabilistic binding to the detachment behavior of this experimental system which was designed to minimize experimental and theoretical complications. This work also corrects an error in the numerical solution of the probabilistic model of receptor-mediated cell attachment and detachment developed previously (Cozens-Roberts, C., D. A. Lauffenburger, and J. A. Quinn. 1990. *Biophys. J.* 58:841–856).

Measurement of the population distribution of the number of receptors per bead has enabled us to explicitly consider the effect of receptor number heterogeneity within the cell-surface contact area. A deterministic framework that incorporates receptor number heterogeneity qualitatively and quantitatively accounts in large part for the model cell detachment data. Using measured and estimated parameter values for the model cell system, we estimate that about 90% of the observed kinetic detachment behavior originates from heterogeneity effects, while about 10% is due to probabilistic binding effects. In general, these relative contributions may differ for other systems.

INTRODUCTION

For proper function, cells of higher organisms must be able to dynamically attach to and detach from other cells, extracellular matrix components, and synthetic materials. Cells use receptor-ligand interactions to facilitate attachment and detachment. Cell adhesion occurs in a wide range of physiological phenomena including the inflammatory response and cancer metastasis (3). A basic understanding of cell adhesion has also encouraged the development of several biotechnological applications. For example, cell affinity chromatography exploits the biochemical specificity of receptor-ligand bonds to isolate one specific cell type from a heterogeneous pool of cells (4–5).

Deterministic kinetic models were first developed to predict the conditions under which adhesion between a cell and a surface would take place (6–8). These models were extended to describe a homogeneous population of cells interacting uniformly with a homogeneous surface. The deterministic balance equation predicts ideal, "all-or-none" behavior: either "all" the cells are attached via receptors to the ligand-coated surface or "none" of the cells are attached. Cozens-Roberts et al. (1) applied this deterministic framework to analyze experimental adhesion data for antibody-coated latex beads on an antigen-coated glass surface. This deterministic model was unable to account for transient detachment observations during which a fraction of the bead population progressively detached rather than all of the beads detaching at once or none of the beads detaching.

Deviations from ideal, all-or-none behavior may be attributed to one or several causes. First, receptor and ligand heterogeneities may influence the system. In a physiological setting, cells may vary in size and may differ in the number and type of receptors exhibited on their surfaces (9–11). Also, the concentration and type of ligands associated with the extracellular matrix and other cells may vary depending on tissue type and other factors (12–13). As a result of these heterogeneities, cell-surface interactions among cells may not be the same; these differences may affect the detachment behavior of a population of cells. Second, since the number of reacting molecules between a cell and its adjacent surface is small, probabilistic reaction rates exist and may influence the macroscopic dynamics of the system (14).

In this paper, we provide a summary of possible heterogeneities and indicate which contributions are likely to be significant in the experimental system of Cozens-Roberts et al. (1). In light of fluorescence flow cytometry measurements of the distribution of the number of receptors linked to latex beads, we explicitly consider nonideal behavior due to receptor number heterogeneity. The quantitative predictions of the deterministic model incorporating receptor number heterogeneity are consistent with the experimental observations of Cozens-Roberts et al. (1). This work is the first quantitative attempt to incorporate the inherent heterogeneities of an experimental biological system into an adhesion model.

The deviation from nonideal behavior resulting from the probabilistic nature of kinetic association and dissociation steps between receptors and ligands was developed by Cozens-Roberts et al. (2) to study cell attachment and detachment kinetics. Their calculations suggested that probabilistic binding effects could be the primary explanation for experimentally observed trends (1). However, a lack of experimental data on nonidealities stemming from heterogeneities prevented a firm conclusion from being drawn. Moreover, further consideration of their calculations revealed a

Received for publication 2 October 1992 and in final form 2 April 1993.

0006-3495/93/07/243/10 $2.00

numerical error which alters the qualitative and quantitative predictions of their model. Correct numerical solutions to the probabilistic model, when solved with expected parameter values, do not capture the experimentally observed dynamics of cell detachment.

In summary, receptor number heterogeneity and probabilistic binding both contribute to the nonideal behavior of the experimental detachment data of Cozens-Roberts et al. (1). We look at receptor number heterogeneity in the context of a simple deterministic kinetic model and probabilistic binding effects in a probabilistic model. We estimate the contributions from receptor number heterogeneity and from inherent probabilistic binding effects to the observed kinetic detachment behavior. Finally, we show predictions for a "combined" model that incorporates both factors known to exist. These models contain a minimum set of parameters, most of which are specified by measurement or reasonable estimation. Only the effective binding rate constants elude fairly narrow specification; these values cannot presently be measured for surface-immobilized receptor-ligand pairs.

NOMENCLATURE

a	radius of contact area between bead and surface
$A(\theta)$	drift term of Fokker-Planck equation
$B(\theta)$	diffusion term of Fokker-Planck equation
C	number of receptor-ligand bonds
CV	coefficient of variation
CV_{het}	CV induced by receptor number heterogeneity
CV_{prob}	CV induced by probabilistic binding effects
F_T	applied fluid shear force
F_{Tc}	value of F_T at which half of the beads detach
k_b	Boltzman constant
k_f^o	intrinsic forward rate constant
k_r^o	intrinsic reverse rate constant
k_r	reverse rate constant under flow conditions
N_L	surface concentration of ligand
P	probability density function
P_b	integrated area under the P versus τ_d curve
$P_{b(F)}$	plateau value of P_b
r	bead radius
R_T	number of receptors within the cell-surface contact area
R_{Tc}	number of receptors per bead
S	applied fluid shear stress
S_c	value of S at which half of the beads detach
t_a	attachment time
t_d	detachment time
T	temperature
β	dimensionless applied shear force
β_c	value of β at which $P_{b(F)} = 0.5$
δ	$1/R_T$
γ	receptor-ligand interaction distance
κ	receptor-ligand dimensionless dissociation constant
θ	fraction of bound receptors
$\langle\theta\rangle$	mean fraction of bound receptors
σ^2	variance around $\langle\theta\rangle$
τ_a	dimensionless attachment time
τ_d	dimensionless detachment time
ζ	fraction of adherent beads

REVIEW OF PREVIOUS EXPERIMENTAL WORK

Cozens-Roberts et al. (1, 15) designed an experimental system to isolate the role of receptor-ligand interactions in the adhesion of a cell to a ligand-coated surface. Several reasons motivated those investigators to select receptor-coated latex beads rather than cells. First, they could select only one type of receptor to coat the bead surface and could modulate its surface concentration. Second, cytoskeletal linkages that exist during cell adhesion are eliminated. Third, unlike cells, latex beads do not deform in the presence of fluid shear stress. By selecting latex beads as model cells, a more homogeneous population of "cells" was expected. Other similar design strategies motivated the construction of their experimental system.

Complete descriptions of the Radial-Flow Detachment Assay (RFDA), plate and bead coating procedures, and protocols for attachment and detachment experiments have been presented previously (1). The beads and chamber surface were covalently coated with rabbit anti-goat IgG and goat IgG, respectively. We followed the conclusion of Cozens-Roberts et al. (15) that each rabbit anti-goat IgG receptor had only one binding site because of the covalent immobilization procedure. Detachment runs involved a 30-min incubation of the beads with the surface followed by a 65-min period during which the beads were subject to fluid shear stress. The fraction of adherent beads (ζ) was reported as a function of time for a range of applied fluid shear stress. Fig. 1 shows a typical detachment profile. Two major observations should be noted. First, there is a continuous loss of beads from the surface which slows down asymptotically over time. Second, the fraction of beads remaining attached to the surface at 60 min decreases with increasing applied fluid shear stress. A "plateau" region in the plot of the fraction of adherent beads versus detachment time is defined when less than 2% detachment is seen in the final 15 min of the detachment trial. This criterion for a plateau value was defined in the Radial-

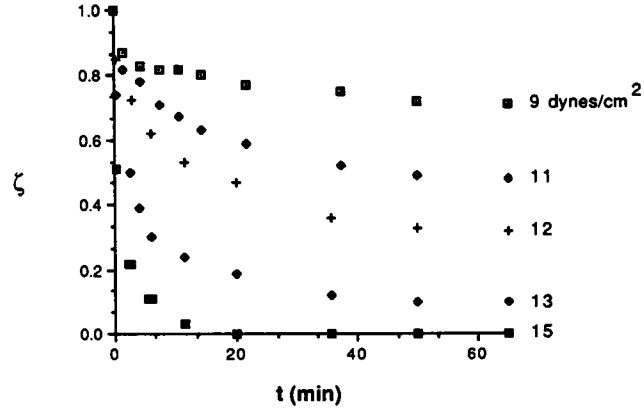

FIGURE 1 Experimental detachment results (1). The fraction of adherent beads (ζ) is plotted versus time for a range of applied fluid shear stress (9–15 dynes/cm^2). Each bead is coated with a receptor concentration of 4.3×10^5 rabbit anti-goat IgG molecules. The surface is coated with goat IgG ligand at a concentration of 4.9×10^{11} 1/cm^2.

Flow Detachment Assay work of Cozens-Roberts et al. (1, 15) and is applied in our modeling work.

Other researchers have also published cell detachment data consistent with the experimental data of Cozens-Roberts et al. (1). McClay et al. (16), Bongrand and Golstein (17), and Hubbard et al. (18) reported that increasing the shear force applied to a population of cells attached to a substrate with specific receptor-ligand bonds decreases the fraction of adherent cells. Hubbard et al. (18) published detachment profiles of the fraction of adherent cells versus time for a range of applied fluid shear stress. Even though different time scales were employed, similar qualitative trends are observed in the detachment data of Hubbard et al. (18) and Cozens-Roberts et al. (1).

A close inspection of the experimental system employed by Cozens-Roberts et al. (1) reveals several possible heterogeneities despite their design efforts. First, the surface concentration of ligand coating the glass surface may be nonuniform. Second, receptor type heterogeneity may be present. Third, the surface concentration of receptors in the cell-surface contact area among individual beads may vary. One source of receptor number variation may be due to differences in size among beads. Fourth, the intrinsic forward and reverse rate constants characterizing receptor-ligand binding may vary from receptor-ligand interaction to interaction. For this system, we assume that ligand number heterogeneity can be neglected since the ligand concentration is in excess of the surface-bound receptor concentration and is therefore not stoichiometrically limiting in receptor-ligand reactions. Although the beads were coated with polyclonal rabbit IgG, variation of receptor type among individual beads is considered negligible because of the random coating procedure. Variation in the surface concentration of receptors in the cell-surface contact area among individual beads does exist; receptor number heterogeneity is examined explicitly in this work. Receptors and ligands are covalently bound to bead and glass surfaces in such a way that a range of conformational interactions, and thus intrinsic forward and reverse rate constants, is expected. However, these variations average out in a cell-surface contact area, and no heterogeneity among beads is expected.

EXPERIMENTAL MEASUREMENTS

Receptor number heterogeneity was estimated from an experimental distribution of the number of IgG receptors covalently linked to latex beads. Polystyrene latex microspheres $(C_8H_8)_n$ with an average diameter of 10 μm ($\pm$1 μm) (Polysciences, Inc., Warrington, PA) were used as model cells. Carbodiimide chemistry was used to covalently link polyclonal rabbit IgG (Zymed Laboratories, San Francisco, CA) via free amine groups to the carboxylated bead surface. The beads and the coating procedure used to link receptors to bead surfaces were identical to those used by Cozens-Roberts et al. (1, 15). The antibody-coated beads were allowed to come to equilibrium for 30 min with a solution of recombinant protein A conjugated with fluorescein isothiocyanate (FITC) (Zymed Laboratories, San Francisco, CA). The population distribution of the number of receptors per bead was determined by flow cytometry by measuring the amount of fluorescein-labeled protein A molecules bound to rabbit IgG on the bead surface. Fluorescence measurements were made on a EPICS model 752 flow cytometer (Coulter Electronics, Hialeah, FL) equipped with an Innova 90-5 argon-ion laser (Coherent, Palo Alto, CA). The voltage was adjusted to keep all samples on a linear scale. Each trial consisted of 5000 beads.

Flow cytometry results are reported for several coating densities as the mean number of total receptors per bead, the standard deviation of that measurement, and the coefficient of variation (CV) (Table 1). The coefficient of variation is defined as the standard deviation divided by the mean (19).

Interference reflection microscopy (IRM) images were taken to validate the geometric estimate of the radius of the cell-surface contact area by Cozens-Roberts et al. (15). Our apparatus consisted of a Nikon Diaphot TMD-EF microscope (Nikon, Inc., Garden City, NY) equipped with a 100 $\times$/1.3 N.A. oil-immersion phase neofluor objective and a Nikon Hg 100-W epifluorescence illuminator (Nikon, Inc., Tokyo, Japan). The filter cube consisted of a 546-nm excitation filter, a 50/50 beam splitter, and a pair of polarizers (Omega Optical, Inc., Brattleboro, VT). Images were viewed with a Newvicon MTI-65 camera (Dage-MTI, Inc., Wabash, MI); images were recorded and analyzed using Biological Detection System image analysis software (Biological Detection System, Inc., Pittsburgh, PA).

In brief, interference reflection microscopy is a technique based on constructive and destructive optical interference patterns (20). As light is reflected off the surface and the bead, waves interfere and create an image containing fringes. These fringes can then be correlated to separation distances between the bead and the surface. IRM images were obtained for a latex bead coated with rabbit IgG (Zymed Laboratories, San Francisco, CA) attached to a glass coverslip coated with protein A (Zymed Laboratories, San Francisco, CA). The dark adhesion spot in the center of an image faded to background irradiance; a series of dark, concentric rings surrounded this dot. Measurement of the radius of the darkened spot of 10 different bead images was 17% ($\pm$3%) of the total bead radius. Following the work of Gingell and coworkers (21–22) for a system with similar refractive indices, the separation distance between the bead and the coverslip of this center adhesion spot is roughly less than 100 nm. Using approximate dimensions of rabbit IgG and protein A, the contact region is estimated as that permitting approach of the bead and surface to within approximately 40 nm (15). Thus, the measurement of the radius of the contact area using IRM is of the same order of magnitude as the geometric estimate and may overestimate the radius of the contact area in which actual receptor-ligand interaction occurs. Thus, the geometric estimate by Cozens-Roberts et al. (15) that the radius of the contact area (0.5 μm) is 10% of total bead radius (5 μm) is valid.

MATHEMATICAL MODELS

Several model frameworks are used to describe and predict transient cell attachment and detachment kinetics. Cells attach via receptors to ligand-coated surfaces in a quiescent fluid; cells detach upon the introduction of fluid shear stress.

Ordinary differential equations describing the deterministic behavior of receptor-mediated cell attachment and detachment have been described (2,

TABLE 1 Flow cytometry measurements of receptor number distribution

Run	Mean number of receptors per bead*	Standard deviation	Coefficient of variation
1	8.1×10^5	2.7×10^5	0.33
2	1.1×10^6	2.4×10^5	0.22
3	1.1×10^6	2.8×10^5	0.25
4	2.1×10^6	5.9×10^5	0.28
5	2.3×10^6	6.2×10^5	0.27
6	2.5×10^6	5.5×10^5	0.22

* The mean number of total receptors per bead, the standard deviation of that measurement, and the coefficient of variation (CV) are listed for six trials (see Experimental Measurements). The CV characterizing the dispersion due to receptor number heterogeneity (CV_{het}) was calculated as 0.26 ± 0.04.

6, 8). Previously, this deterministic model was extrapolated and applied to characterize a population of cells with uniform cell-surface interactions (2). We return to the initial deterministic framework, neglect the assumption of uniform cell-surface interactions, and develop an algorithm that explicitly considers receptor number heterogeneity among beads (see Appendix I).

Complete derivation and description of kinetic population balance equations characterizing the probabilistic nature of receptor-mediated cell attachment and detachment have been described previously (2). The probabilistic nature of these receptor-ligand interactions is captured in the corresponding attachment and detachment Fokker-Planck partial differential equations and associated initial and boundary conditions (see Appendix II).

The effects of receptor number heterogeneity and probabilistic binding are joined in a mathematical model (see Appendix III).

Solutions to the ordinary differential equations were obtained with a classic Runge-Kutta algorithm (23–24). Solutions to the parabolic Fokker-Planck equations were obtained by implementing the subroutine D03PAF from the NAG FORTRAN Library (Numerical Algorithms Group Ltd., Downers Grove, IL). This subroutine applied the method of lines and Gear's integration method (25). Computations were performed on a CRAY Y-MP computer.

Parameter values specific for the receptor (rabbit anti-goat IgG)-ligand (goat IgG) system used in the experimental detachment work of Cozens-Roberts et al. (1) are listed in Table 2. The average number of receptors per bead and the average surface ligand concentration were measured directly by Cozens-Roberts et al. (1). The bead diameter distribution was given by the manufacturer (Polysciences, Inc.). The radius of the cell-surface contact area was previously estimated by geometric arguments (15) and is validated with IRM images. The average number of receptors in the cell-surface contact area was estimated based on the measured number of receptors per bead and on geometric considerations. The value of the receptor-ligand interaction distance (γ) and ranges for the forward and reverse rate constants (k_f^o and k_r^o) were taken from Bell (6) and Cozens-Roberts et al. (2), respectively. At the present time, no methods exist to measure these parameter values. We selected four parameter sets for model calculations. Cases A–D are specified in Table 3.

TABLE 3 Comparisons of CV_{het} and CV_{prob}

CASE*	A	B	C	D
κ	10	1	0.1	0.01
$k_f^o N_L$	1×10^{-3} 1/s	4×10^{-3} 1/s	5×10^{-3} 1/s	1×10^{-2} 1/s
k_r^o	1×10^{-2} 1/s	4×10^{-3} 1/s	5×10^{-4} 1/s	1×10^{-4} 1/s
CV_{het}	CV_{prob}	CV_{prob}	CV_{prob}	CV_{prob}
	0.141	0.0447	0.0141	0.00447
0.22	39%	17%	6.0%	2.0%
	0.141	0.0447	0.0141	0.00447
0.26	35%	15%	5.1%	1.7%
	0.141	0.0447	0.0141	0.00447
0.30	32%	13%	4.5%	1.5%

* Cases A–D contain parameter values within expected ranges (see Table 2). The coefficient of variation induced by probabilistic binding effects (CV_{prob}) was calculated for each case by solving the Fokker-Planck attachment equation which provides the probability distribution used as the initial condition for the Fokker-Planck detachment equation. The mean and standard deviation of this distribution were used to calculate CV_{prob}. Additional parameters not listed above are as follows: t_a = 30 min, R_T = 500, and $N_L = 10^{11}$ 1/cm^2. Flow cytometry studies determined the coefficient of variation induced by receptor number heterogeneity (CV_{het}) as 0.26 ± 0.04. We calculated the weight percentage of the probabilistic dispersion as 100 CV_{prob}/(CV_{prob} + CV_{het}) for each case for each value of CV_{het}.

RESULTS AND DISCUSSION

We first estimate dispersions caused by receptor number heterogeneity and by probabilistic binding effects. To provide an estimate of the probabilistic binding contribution, corrected numerical results to the probabilistic Fokker-Planck attachment equation are given. The relative importance of each dispersion is estimated as a coefficient of variation (CV) which is defined as the standard deviation divided by the mean (19). The contributions to detachment behavior from these two effects are compared. Second, we present detachment profiles based on the incorporation of receptor number heterogeneity into a simple deterministic model. Third, we demonstrate that for expected parameter ranges, numerical results for the probabilistic detachment model inadequately predict detachment data. Since receptor number heterogeneity and probabilistic binding effects are both shown to affect experimental detachment kinetics, we develop a mathematical framework that incorporates both components. The deterministic, probabilistic, and combined models are solved for established parameter values and are compared with experimental detachment data (1).

Table 1 presents experimental values obtained by fluorescence flow cytometry of the mean number of total receptors per bead and the coefficient of variation (CV) of this measurement. The average number of receptors per bead reported by Cozens-Roberts et al. (1) is of the same order of magnitude as these flow cytometry results. Since the bead coating technique used in this work was the same as that used by those investigators, we assume this dispersion is a valid

TABLE 2 Parameters characterizing the experimental system of Cozens-Roberts et al. (1)

	Symbol	Value	Reference
Measured parameters*			
Average receptor number	R_{TC}	4.3×10^5	1
Average ligand concentration	N_L	4.9×10^{11} 1/cm^2	1
Bead diameter	$2r$	10 ± 1 μm	Text
Estimated parameters			
Radius of contact area	a	0.5 μm	15, Text
Average R_{TC} in contact area	R_T	500	Text
Interaction distance	γ	0.5 nm	6
Estimated parameter ranges			
Ligand concentration	N_L	10^{11}–10^{12} 1/cm^2	2
Forward rate constant	k_f^o	10^{-14}–10^{-12} cm^2/s	2
Reverse rate constant	k_r^o	10^{-4}–10^{-2} 1/s	2

* Beads were coated with rabbit anti-goat IgG; the surface was coated with goat IgG. Parameter values not determined in this text have been taken from sources listed in the References.

estimate for the receptor number heterogeneity present in their experimental system. We assume that the uneven distribution of receptors on each bead surface is insignificant compared to the variation in receptor number among beads so that an identical CV characterizes the dispersion over whole and fractions of bead surfaces. We thus describe the CV induced by receptor number heterogeneity within the contact area (CV_{het}) as 0.26 ± 0.04 and use this dispersion to directly consider the effect of receptor number heterogeneity. As mentioned earlier, receptor number heterogeneity may be induced by differences in size among beads. Product specifications of the polystyrene latex microspheres used as model cells are as follows: average diameter = 10 μm and standard deviation = 1 μm. Assuming constant receptor number per unit area, the CV characterizing receptor number heterogeneity based solely on size distribution is 0.20 (26). Bead size distribution accounts for greater than 75% of the experimentally measured dispersion. Other factors may also contribute to the distribution of receptor number within the contact area. Therefore, the value of CV_{het} measured with fluorescence flow cytometry is reasonable.

The dispersion induced by probabilistic binding was estimated by solving the Fokker-Planck attachment equation which provided the probability distribution used as the initial condition for the Fokker-Planck detachment equation. The Fokker-Planck attachment equation was solved with appropriate initial and boundary conditions and with the receptor-ligand dimensionless dissociation constant (κ), dimensionless attachment time (τ_a), and number of receptors within the cell-surface contact area (R_T) specified (see Appendix II and Eqs. A5–A8). The probability (P) of being attached with θ fraction of bound receptors varies as a function of the dimensionless dissociation constant (κ) (Fig. 2). McQuarrie's analysis of a similar kinetic system confirms the probability distributions shown in Fig. 2 (27). McQuarrie's solution is a normal probability distribution with a mean and variance written in analytic form. The analogous expressions for the mean fraction of bound receptors ($\langle\theta\rangle$) and the variance (σ^2) around this mean are as follows:

$$\langle\theta\rangle = \frac{1}{(1+\kappa)}(1 - e^{-(1+\kappa)\tau_a}) \quad (1)$$

$$\sigma^2 = \frac{1}{R_T}\frac{1}{(1+\kappa)^2}\left[\kappa(1 - e^{-(1+\kappa)\tau_a}) + e^{-(1+\kappa)\tau_a} - e^{-2(1+\kappa)\tau_a}\right]. \quad (2)$$

As predicted, each computationally generated solution is a normal distribution with a mean and variance that agree with McQuarrie's analytical solution. We did not transform this normal distribution into a lognormal distribution as was done previously by Cozens-Roberts et al. (2). The mean and standard deviation of this normal distribution were used to calculate the coefficient of variation induced by probabilistic binding effects (CV_{prob}).

The variance given in Eq. 2 is different from that published by Cozens-Roberts et al. (2) by the factor, $1/R_T$. The value of CV_{prob} is inversely proportional to the square root of the number of receptors within the cell-surface contact area. Consequently, the larger the value of R_T, the smaller the value that CV_{prob} is.

Table 3 lists CV_{het} and CV_{prob} for four parameter selections (Cases A–D) with R_T set as 500. In addition, the weight percentage of the probabilistic contribution was calculated as $100CV_{prob}/(CV_{prob} + CV_{het})$ and is included in Table 3. For reasonable parameter selections, the CV_{prob} ranges from 0.004 to 0.14. From these calculations, we estimate that the probabilistic binding contribution could range from approximately 1 to 40%. This analysis assumes a uniform distribution of stress on all bonds in the cell-surface contact area. In contrast, other researchers assume that only perimeter bonds are stressed (28). In that light, our estimation of the role of probabilistic binding effects should be treated as a lower bound.

To understand detachment behavior, we deemed it important to solve the deterministic model incorporating receptor number heterogeneity, the probabilistic model, and the combined model that joins receptor number heterogeneity and probabilistic binding effects.

The effects of receptor number heterogeneity are considered in the context of a simple deterministic model (see Appendix I). Ordinary differential equations were solved and are presented as the time evolution of the area under the probability curve (P_b). The detachment profiles of Fig. 3 were generated with parameter values of Case C (κ = 0.1). The mean number of receptors within the cell-surface contact area was set as 500 with CV_{het} = 0.22. The area under the probability curve (P_b) is analogous to the fraction of adherent beads (ζ) presented in the experimental detachment data. Numerical solutions to the deterministic model incorporating receptor number heterogeneity for all cases for all listed CV_{het} values of Table 3 are qualitatively identical to Fig. 3.

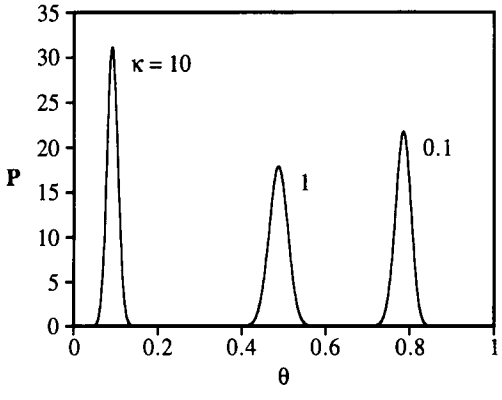

FIGURE 2 Results of the Fokker-Planck probabilistic attachment equation. The probability density function (P) is plotted versus the fraction of bound receptors (θ) for a range of dimensionless dissociation constants (κ). The parameters are as follows: R_T = 500, $k_f^0 = 10^{-14}$ cm²/s, $N_L = 10^{11}$ 1/cm², $k_r^0 = 10^{-4}$, 10^{-3}, 10^{-2} 1/s (κ = 0.1, 1, 10), and t_a = 30 min (τ_a = 1.8). The area under each trace is normalized to 1.

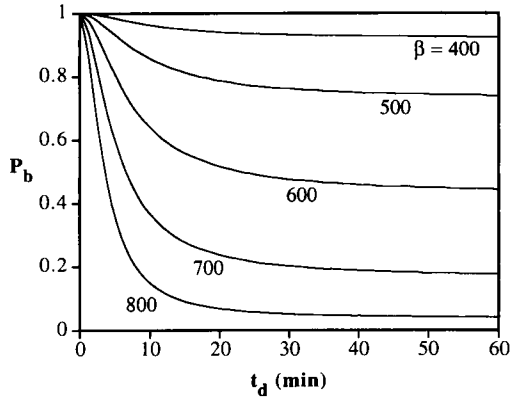

FIGURE 3 Results of the deterministic model incorporating receptor number heterogeneity. The area under the probability curve (P_b) is plotted versus time (t_d) for a range of fluid shear forces (β). The mean number of receptors within the contact area was set at 500; CV_{het} was chosen as 0.22. Parameter values listed as Case C are as follows: $k_f^o = 5 \times 10^{-14}$ cm^2/s, $N_L = 10^{11}$ 1/cm^2, $k_r^o = 5 \times 10^{-4}$ 1/s ($\kappa = 0.1$), $t_a = 30$ min ($\tau_a = 9$), and $t_d = 0$–60 min ($\tau_d = 0$–18).

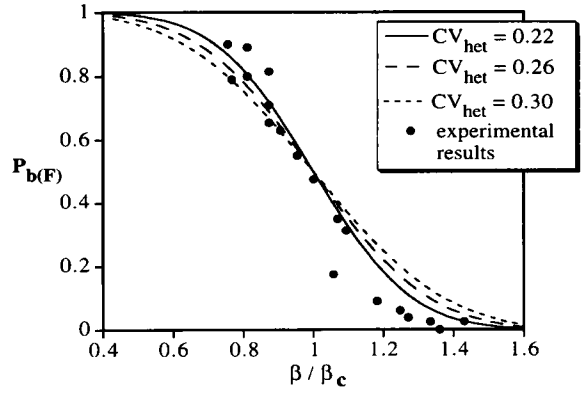

FIGURE 4 Comparison of experimental data with the deterministic model incorporating receptor number heterogeneity. The plateau values of P_b ($P_{b(F)}$) and of the fraction of adherent beads are analogous. Also analogous are the ratios of β/β_c (where β_c is the value of β at which $P_{b(F)} = 0.5$) and F_T/F_{Tc} (where F_{Tc} is the value of fluid shear force at which half of the beads detach). The traces of $P_{b(F)}$ versus β/β_c are shown with the transformed experimental data. Parameter values are listed in Fig. 3. Model results are taken from Fig. 3 ($CV_{het} = 0.22$) and from two figures that are not shown ($CV_{het} = 0.26$ and $CV_{het} = 0.30$). Experimental points are taken from Fig. 1 and other previously published results (1).

All model detachment profiles show some immediate detachment and a plateau region as time approaches 60 min. The general nature of these detachment profiles is compared with reported RFDA data (see Fig. 1). Numerical solutions to the deterministic model incorporating receptor number heterogeneity qualitatively and quantitatively predict experimental detachment profiles.

An additional check is made between model predictions and experimental data. The plateau values of P_b ($P_{b(F)}$) and of the fraction of adherent beads are analogous. Also analogous are the ratios of β/β_c (where β_c is the value of β at which $P_{b(F)} = 0.5$) and F_T/F_{Tc} (where F_{Tc} is the value of fluid shear force (F_T) at which half of the beads detach). The graph of $P_{b(F)}$ versus β/β_c for the parameters listed as Case C for CV_{het} values of 0.22, 0.26, and 0.30 is shown with transformed experimental data (Fig. 4). As the magnitude of CV_{het} is decreased, the curve becomes more steep. When $CV_{het} = 0$ and receptor number heterogeneity is effectively eliminated, this model collapses to the preliminary deterministic model developed by Cozens-Roberts et al. (2), and a step change (i.e., all-or-none behavior) is predicted.

$P_{b(F)}$ versus β/β_c curves were generated for Cases A, B, and D (figures not shown). For a specified CV_{het}, altering κ and $k_f^o N_L$ does not affect the shape of the curve. The magnitude of CV_{het} is the primary determinant of the fit of the experimental data for the deterministic model incorporating receptor number heterogeneity. Our work indicates that the curve with $CV_{het} = 0.22$ is a good predictor of the experimental data published by Cozens-Roberts et al. (1).

Correct numerical solutions to the Fokker-Planck probabilistic detachment equation are presented as the time evolution of the area under the probability curve (P_b) (see Appendix II and Eqs. A9–A12). The detachment profiles of Fig. 5 were generated with parameter values listed as Case C ($\kappa = 0.1$) and Case A ($\kappa = 10$). Again, the area under the probability curve (P_b) can be directly compared with the fraction of adherent beads (ζ). As the dimensionless applied shear force (β) increases, the fraction of cells remaining attached to the surface decreases for a given t_d. The parameter values for Cases A and C specify $\langle\theta\rangle$ for the initial condition for the Fokker-Planck detachment equation as 0.0909 and 0.9090, respectively. As the mean fraction of bound receptors ($\langle\theta\rangle$) given as the initial condition increases, the dimensionless shear force (β) required to detach the same fraction of cells increases. In other words, the greater the number of receptor-ligand bonds, the stronger the applied fluid shear force must be to detach the same fraction of cells. This trend also can be viewed from another perspective. The increase in the value of $\langle\theta\rangle$ as an initial condition is correlated with a decrease in the dimensionless rate constant (κ). Therefore, as the affinity between the receptor and ligand increases (κ decreases), a greater fluid shear force is required to detach the same fraction of cells. The same observations linking receptor-ligand affinity, the initial mean fraction of bound receptors, and the magnitude of fluid shear force can be made for the deterministic model incorporating receptor number heterogeneity.

The general nature of these two probabilistic detachment profiles is compared with reported RFDA data (see Fig. 1). The profile with $\kappa = 0.1$ predicts a minimum lag time before detachment of approximately 8 min (see Fig. 5 *A*). In addition, no plateau behavior is observed at 60 min. The RFDA detachment profiles show a negligible lag time and plateau behavior as defined earlier. All possible combinations of expected parameters were checked with respect to these two features; the profiles shown in Fig. 5 *A* are the best prediction. A lag time is still observed, and a plateau region is not reached. Therefore, the conclusion of Cozens-Roberts et al. (1) that a purely probabilistic model can make successful quantitative predictions of detachment behavior is not upheld.

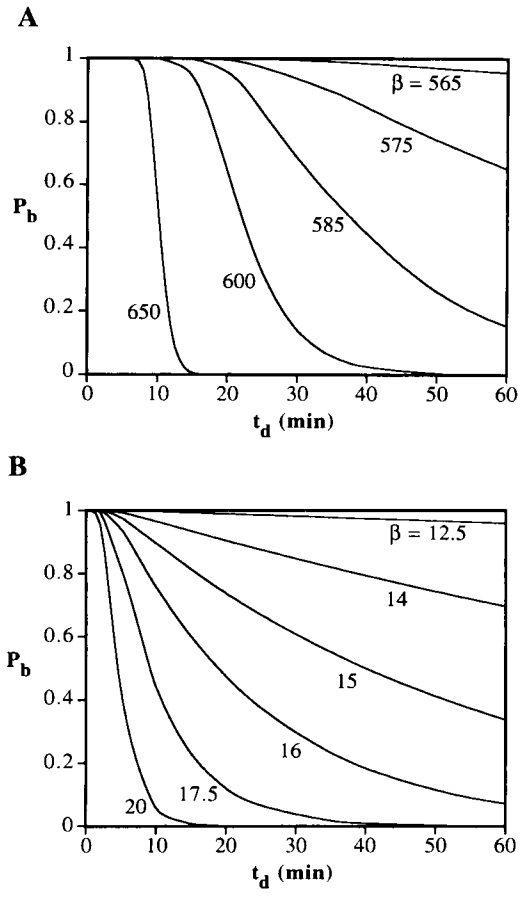

FIGURE 5 Results of the Fokker-Planck probabilistic detachment equation. The area under the probability curve (P_b) is plotted versus time (t_d) for a range of dimensionless fluid shear forces (β). (*A*) Parameter values listed as Case C are as follows: $R_T = 500$, $k_f^o = 5 \times 10^{-14}$ cm²/s, $N_L = 10^{11}$ 1/cm², $k_r^o = 5 \times 10^{-4}$ 1/s ($\kappa = 0.1$), $t_a = 30$ min ($\tau_a = 9$), and $t_d = 0$–60 min ($\tau_d = 0$–18). These parameters specify the mean fraction of bound receptors ($\langle\theta\rangle$) for the initial condition for the Fokker-Planck detachment equation as 0.9090. (*B*) Parameter values listed as Case A are as follows: $R_T = 500$, $k_f^o = 10^{-14}$ cm²/s, $N_L = 10^{11}$ 1/cm², $k_r^o = 10^{-2}$ 1/s ($\kappa = 10$), $t_a = 30$ min ($\tau_a = 1.8$), and $t_d = 0$–60 min ($\tau_d = 0$–3.6). These parameters specify $\langle\theta\rangle$ for the initial condition for the Fokker-Planck detachment equation as 0.0909.

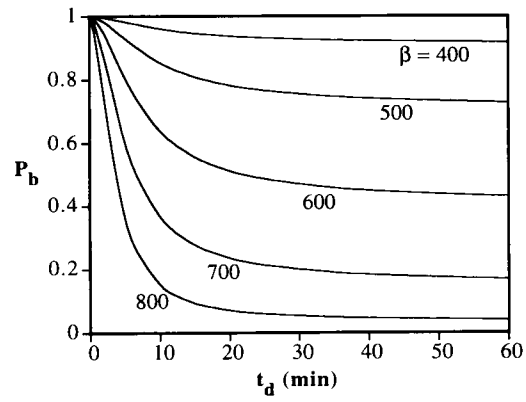

FIGURE 6 Results of the combined model incorporating receptor number heterogeneity and probabilistic binding effects. The area under the probability curve (P_b) is plotted versus time (t_d) for a range of fluid shear forces (β). The mean number of receptors within the contact area was set at 500; CV_{het} was chosen as 0.22. Parameter values listed as Case C are as follows: $k_f^o = 5 \times 10^{-14}$ cm²/s, $N_L = 10^{11}$ 1/cm², $k_r^o = 5 \times 10^{-4}$ 1/s ($\kappa = 0.1$), $t_a = 30$ min ($\tau_a = 9$), and $t_d = 0$–60 min ($\tau_d = 0$–18). The weight percentage of the probabilistic contribution is estimated as 6%.

Finally, numerical solutions to the combined model overlaying probabilistic binding effects onto the deterministic model incorporating receptor number heterogeneity were determined (see Appendix III). The time evolution of the area under the probability curve (P_b) is shown for the parameter values of Case C (Fig. 6). The mean number of receptors within the contact area was set as 500 with $CV_{het} = 0.22$. Each detachment profile shows some immediate detachment and a plateau region as time approaches 60 min. The probabilistic contribution to the deviations from all-or-none behavior is predicted to be 6%. We compared $P_{b(F)}$ versus β/β_c plots for the solution of the deterministic model incorporating receptor number heterogeneity and for the solution of the combined model; these two curves were the same (figure not shown).

Both the deterministic model incorporating receptor number heterogeneity and the combined model were solved for Case A with $CV_{het} = 0.28$ (Fig. 7, *A* and *B*). The detachment profiles of the deterministic model predict plateau solutions as time approaches 60 min. Including probabilistic effects prevents plateau behavior (see Fig. 7 *B*). Here, the probabilistic binding contribution to the deviations from all-or-none behavior is predicted to be 33%. A plot of $P_{b(F)}$ versus β/β_c for the deterministic and combined model solutions indicates that incorporating probabilistic binding effects relaxes the steepness of the curve (Fig. 7 *C*). This plot serves as an important test of the assumption that the calculation of the weight percentage of the probabilistic contribution is a valid tool in assessing the role of probabilistic binding effects.

Values of κ from Cases A–D span three orders of magnitude. Although each of these cases contains parameters within reasonable ranges, we sought to narrow this spread. One approach is to compare published affinity values to our model values. Based on modeling and experimental work, Cozens-Roberts et al. (15) calculated the affinity constant of formation between the receptor (rabbit anti-goat IgG) and the ligand (goat IgG) as 1.4×10^{-10} cm². This affinity constant corresponds to $\kappa = 0.07$ for $N_L = 1 \times 10^{11}$ 1/cm². Based on theoretical calculations, Perelson et al. (29) estimated the affinity constant of a similar system as 2.9×10^{-10} cm². This affinity constant corresponds to $\kappa = 0.03$ for $N_L = 1 \times 10^{11}$ 1/cm². To date, no researcher has directly measured κ for surface-immobilized receptor-ligand pairs. Even flow cytometry measurements of k_f^o and k_r^o are not applicable since these measurements determine fluid phase rate constants rather than surface-bound rate constants. Thus, we suggest $0.01 \leq \kappa \leq 0.1$ as a likely constraint.

A second approach is to compare the experimental force exerted on a bead with the force predicted by our model. The total force (F_T) exerted by the passing fluid on an adherent

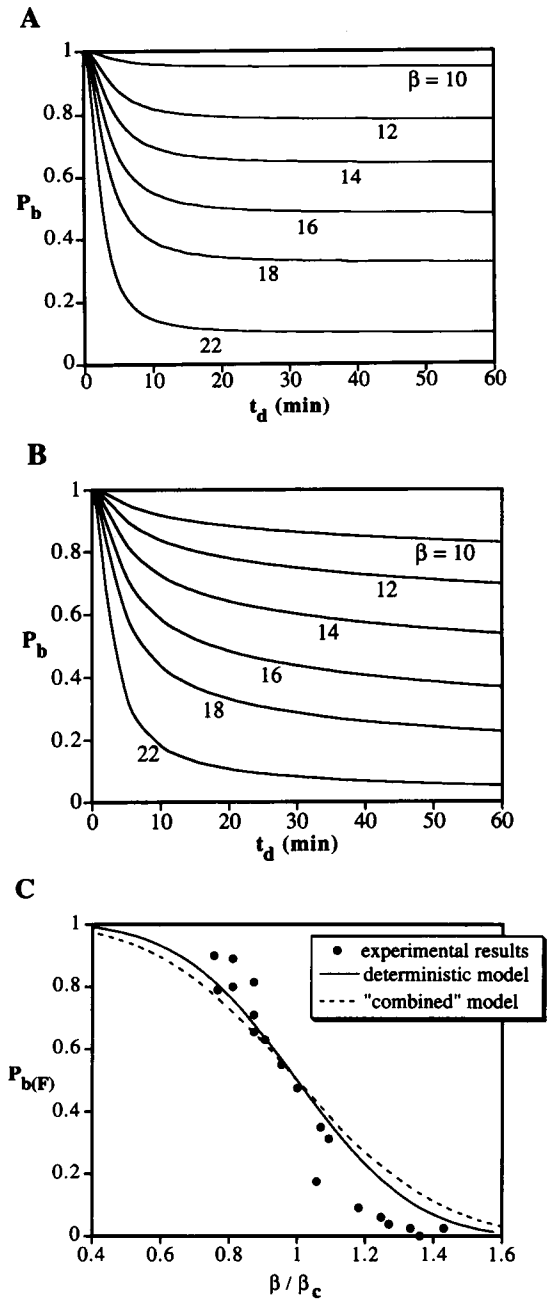

FIGURE 7 Results for the deterministic and combined models that demonstrate that probabilistic binding effects can contribute to detachment behavior. The weight percentage of the probabilistic binding contribution is estimated as 33%. Parameter values listed as Case A are as follows: R_T = 500, k_f° = 10^{-14} cm²/s, N_L = 10^{11} 1/cm², k_r° = 10^{-2} 1/s (κ = 10), t_a = 30 min (τ_a = 1.8), and t_d = 0–60 min (τ_d = 0–3.6). The mean number of receptors within the contact area was set at 500; CV_{het} was chosen as 0.28. (*A*) Results of the deterministic model incorporating receptor number heterogeneity. The area under the probability curve (P_b) is plotted versus time (t_d) for a range of fluid shear forces (β). (*B*) Results of the combined model. The area under the probability curve (P_b) is plotted versus time (t_d) for a range of fluid shear forces (β). (*C*) Comparison of experimental data with the deterministic model and with the combined model. The plateau values of P_b ($P_{b(F)}$) and of the fraction of adherent beads are analogous. Also analogous are the ratios of β/β_c (where β_c is the value of β at which $P_{b(F)}$ = 0.5) and F_T/F_{Tc} (where F_{Tc} is the value of fluid shear force at which half of the beads detach). The traces of $P_{b(F)}$ versus β/β_c are shown with the transformed experimental data from Fig. 1 and other previously published results (1). Model results are taken from Fig. 7, *A* and *B*.

bead is given with the following equation:

$$F_T = \frac{110Sr^3}{a} \tag{3}$$

where S is the fluid shear stress; r is the radius of the bead; and a is the radius of the contact area (15). These calculations were done for mean r and a values and for "critical" values (labeled with subscript "c"). In conjunction with their detachment profiles, Cozens-Roberts et al. (1) reported S_c, the fluid shear stress at which half of the beads detach, as 11 dyne/cm². Therefore, F_{Tc} is estimated as 3.0×10^{-3} dyne. Our model includes the total force exerted on the receptor-ligand bonds by the fluid with the following equation:

$$F_T = \frac{\beta k_b T}{\gamma} \tag{4}$$

where β is the dimensionless applied shear force; k_b is the Boltzman constant; T is the temperature; and γ is the receptor-ligand interaction distance. Our model does not account for nonspecific binding between a receptor-coated bead and a surface because, for the experimental system at hand, it was shown to be negligible (15). In general, this contribution to the force should be considered. β_c, the value of β at which $P_{b(F)}$ = 0.5, was determined for the detachment model incorporating receptor number heterogeneity for the four cases. Theoretical F_{Tc} values for $0.01 \leq \kappa \leq 0.1$ are within an order of magnitude of the experimental force estimate. Theoretical F_{Tc} values for higher κ values underpredict the experimental force. Again, this points to the likelihood that κ falls at the lower end of the expected parameter range.

In summary, both receptor number heterogeneity and probabilistic binding affect cell detachment behavior. A realistic, dynamic model must incorporate both. A simple deterministic model incorporating receptor number heterogeneity satisfactorily accounts for most of the experimental data on detachment kinetics. We believe that model solutions with parameter sets for which $0.01 \leq \kappa \leq 0.1$ are most reasonable based on physical and kinetic considerations. In this parameter range, we estimate that probabilistic binding effects contribute less than 10% to the character of the detachment profiles. Therefore, we conclude that receptor number heterogeneity is the primary cause of deviations from ideal, all-or-none behavior reported in the experimental system of Cozens-Roberts et al. (1). In general, the relative contributions of population heterogeneities and probabilistic binding effects may vary for different systems.

More complicated models may be useful for deeper analysis of detachment experiments. A promising example is work by Hammer and Apte (30). However, a healthy tension always exists between rigor and simplicity, which can only be settled by utility to the problem at hand. We believe that our application of the simplest model that includes both heterogeneity and probabilistic binding considerations, and requires a limited set of unknown parameters, has provided

novel and helpful insight concerning the relative contribution of these effects in a relatively well-characterized experimental system.

APPENDICES

Appendix I: Deterministic model

A cell coated with one class of receptors interacts with surface-bound ligands to form receptor-ligand complexes. R_T receptors are available within the cell-surface contact area. The surface concentration of ligand (N_L) is in excess of the surface concentration of receptors. Therefore, N_L is not depleted as C receptor-ligand bonds are established. Receptor-ligand binding is characterized by intrinsic forward and reverse rate constants (k_f^o and k_r^o). The model allows a cell to attach in quiescent fluid; however, cell detachment is accomplished by the introduction of fluid shear stress. Attachment time is given as t_a; detachment time is given as t_d.

Cozens-Roberts et al. (2) applied deterministic conservation equations to predict transient cell attachment and detachment kinetics. The following equations were developed to describe the interaction of one cell with a ligand-coated surface. The dimensionless differential equation for cell attachment relates the fraction of bound receptors (θ) to the attachment time (τ_a) and receptor-ligand dissociation constant (κ) with the following equation:

$$\frac{d\theta(\tau_a)}{d\tau_a} = 1 - \theta(\tau_a) - \kappa\theta(\tau_a) \tag{A1}$$

where

$$\tau_a = k_f^o N_L t_a \qquad \kappa = \frac{k_r^o}{k_f^o N_L} \qquad \theta = \frac{C}{R_T}.$$

The initial condition is as follows:

$$\theta(0) = 0. \tag{A2}$$

In order to incorporate the effect of fluid shear force on detachment dynamics, we implemented the expression developed by Bell (6) for the reverse rate constant:

$$k_r = k_r^0 \exp\left[\frac{\gamma F_T}{k_b T C}\right] \tag{A3}$$

where γ is the receptor-ligand interaction distance, F_T is the total force exerted on bonds by the fluid, k_b is the Boltzman constant; and T is the temperature. The dimensionless differential equation for cell detachment relates the fraction of bound receptors (θ) to the detachment time (τ_d), dissociation constant (κ), and fluid shear force (β) with the following equation:

$$\frac{d\theta(\tau_d)}{d\tau_d} = 1 - \theta(\tau_d) - \kappa\theta(\tau_d)\exp\left[\frac{\beta\delta}{\theta(\tau_d)}\right] \tag{A4}$$

where

$$\tau_d = k_f^o N_L t_d \qquad \beta = \frac{\gamma F_T}{k_b T} \qquad \delta = \frac{1}{R_T}.$$

The initial condition for the deterministic detachment equation is the numerical result of the appropriate deterministic attachment equation (Eq. A1).

We developed an algorithm which incorporates the effect of receptor number heterogeneity into these basic attachment and detachment equations. A probability distribution of the number of receptors within the cell-surface contact area was established based on flow cytometry experiments (Fig. A1). Several steps were needed to generate a model prediction that can be readily compared with an experimental RFDA. First, the attachment equation was solved for a specified κ and τ_a to generate an initial condition that completely specifies the detachment problem statement. Note that the solution to the attachment equation is not dependent on the value of R_T. Second, the detachment equation was solved for the fraction of bound receptors (θ) as a function of τ_d for specified values of R_T, κ, and β. If θ was greater than δ, the probability of being attached was 1. If θ was less than δ, the probability of being attached was 0. Therefore, the θ versus τ_d plot was converted into a graph relating the probability of remaining attached (P_b) to τ_d. The detachment equation was solved repeatedly for all values of R_T that contribute to the probability distribution of Fig. A1. Each P_b versus τ_d graph was weighted in accordance with the established distribution to generate one constant β detachment curve. Finally, the plot of P_b versus τ_d was converted to a plot of P_b versus t_d. P_b is analogous to the fraction of adherent beads (ζ) presented in an experimental RFDA profile.

Appendix II: Probabilistic model

Cozens-Roberts et al. (2) developed kinetic population balance equations and their corresponding Fokker-Planck equations to characterize the probabilistic nature of receptor-mediated cell attachment and detachment. Following the parameter definitions in Appendix I, the dimensionless Fokker-Planck equation for cell attachment relates the probability density function (P) to the fraction of bound receptors (θ), attachment time (τ_a), and receptor-ligand dissociation constant (κ) with the following equation:

$$\frac{\partial P(\theta,\tau_z)}{\partial \tau_a} = -\frac{\partial}{\partial\theta}[A(\theta)P(\theta,\tau_a)] + \frac{1}{2}\frac{\partial^2}{\partial\theta^2}[B(\theta)P(\theta,\tau_a)] \tag{A5}$$

where

$$A(\theta) = 1 - \theta - \kappa\theta \qquad B(\theta) = [1 - \theta + \kappa\theta]\delta \tag{A6}$$

$$\tau_a = k_f^o N_L t_a \qquad \kappa = \frac{k_r^o}{k_f^o N_L} \qquad \theta = \frac{C}{R_T} \qquad \delta = \frac{1}{R_T}.$$

Boundary and initial conditions that accurately reflect the physics of the system are given below:

$$A(\theta)P(\theta,\tau_a) - \frac{1}{2}\frac{\partial}{\partial\theta}[B(\theta)P(\theta,\tau_a)] = 0 \qquad \theta = 0, \quad \theta = 1 \tag{A7}$$

$$P(\theta,0) = 1. \tag{A8}$$

We incorporated the expression developed by Bell (6) for the reverse rate constant (Eq. A3) into the dimensionless Fokker-Planck equation for cell detachment which relates the probability density (P) to the fraction of bound receptors (θ), detachment time (τ_d), dissociation constant (κ), and fluid shear force (β) with the following equation:

$$\frac{\partial P(\theta,\tau_d)}{\partial \tau_d} = -\frac{\partial}{\partial\theta}[A(\theta)P(\theta,\tau_d)] + \frac{1}{2}\frac{\partial^2}{\partial\theta^2}[B(\theta)P(\theta,\tau_d)] \tag{A9}$$

where

$$A(\theta) = 1 - \theta - \kappa\theta\exp\left[\frac{\beta\delta}{\theta}\right]$$

$$B(\theta) = \left[1 - \theta + \kappa\theta\exp\left[\frac{\beta\delta}{\theta}\right]\right]\delta \tag{A10}$$

$$\tau_d = k_f^o N_L t_d \qquad \beta = \frac{\gamma F_T}{k_b T}.$$

Appropriate boundary conditions are given below:

$$\delta^2\frac{\partial P(\theta,\tau_d)}{\partial\theta} - \delta[\beta - 3]P(\theta,\tau_d) = 0 \qquad \theta=\delta \tag{A11}$$

$$A(\theta)P(\theta,\tau_d) - \frac{1}{2}\frac{\partial}{\partial\theta}[B(\theta)P(\theta,\tau_d)] = 0 \qquad \theta = 1. \tag{A12}$$

The initial condition for the Fokker-Planck detachment equation is the numerical result of the appropriate attachment equation (Eq. A5) with selected parameter values.

Several steps were needed to generate a model prediction that can be readily compared with an experimental RFDA. First, κ, τ_a, R_T, τ_d, and β were set. Second, an attachment run generated an initial condition to completely specify the detachment problem statement. This normal distribution was not transformed into a lognormal distribution as was done previously

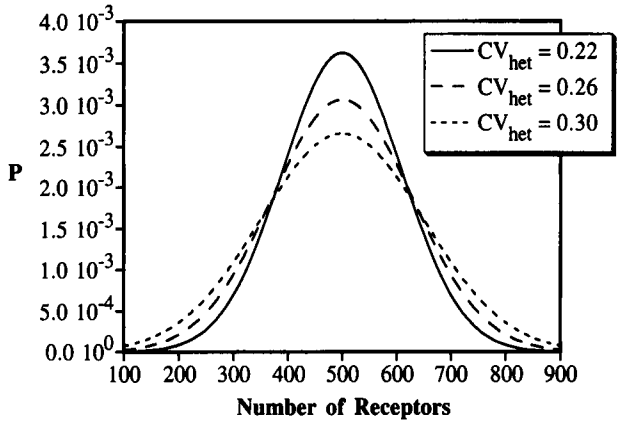

FIGURE A1 Scaled flow cytometry measurements. The normal probability distribution of the number of receptors was scaled so that the mean number of receptors in the cell-surface contact area was 500. The coefficient of variation induced by receptor number heterogeneity (CV_{het}) was calculated as 0.26 ± 0.04.

by Cozens-Roberts et al. (2). Third, the Fokker-Planck detachment equation was solved for the probability density (P) as a function of the fraction of bound receptors (θ) for a range of specified τ_d values. Fourth, for each τ_d, the area under the probability curve (P_b) was computed and plotted as a function of τ_d. Finally, the plot of P_b versus τ_d was converted to a plot of P_b versus t_d. P_b is analogous to the fraction of adherent beads (ζ) presented in an experimental RFDA profile.

Appendix III: Combined model

The following algorithm was used to generate detachment profiles that include both receptor number heterogeneity and probabilistic binding effects. First, a probability distribution of the number of receptors within the cell-surface contact area was established based on flow cytometry experiments (Fig. A1). A Fokker-Planck attachment trial was run for a specified R_T value. Then, the Fokker-Planck equation for detachment was solved for the time evolution of the area under the probability curve (P_b) for that R_T value for several specified β values (see Appendix I). These two computational steps were repeated for all R_T values that contribute to the receptor number distribution. Finally, for each β value, the contribution from each unique R_T detachment curve was weighted in accordance with the established distribution of Fig. A1 to generate one constant β detachment curve. Each theoretical detachment curve is analogous to an experimental RFDA profile.

We appreciate the technical support from the National Center for Supercomputing Applications at the University of Illinois at Urbana-Champaign. Financial support from a National Science Foundation Graduate Fellowship (to A. Saterbak) and from an unrestricted grant from CellPro, Inc. (to D. A. Lauffenburger) is gratefully acknowledged.

REFERENCES

1. Cozens-Roberts, C., D. A. Lauffenburger, and J. A. Quinn. 1990. Receptor-mediated cell attachment and detachment kinetics. II. Experimental model studies with the Radial-Flow Detachment Assay. *Biophys. J.* 58:857–872.
2. Cozens-Roberts, C., D. A. Lauffenburger, and J. A. Quinn. 1990. Receptor-mediated cell attachment and detachment kinetics. I. Probabilistic model and analysis. *Biophys. J.* 58:841–856.
3. Alberts, B., D. Bray, J. Lewis, M. Raff, K. Roberts, and J. D. Watson. 1989. Molecular biology of the cell. Garland Publishing, Inc., New York. 1219 pp.
4. Hertz, C. M., D. J. Graves, D. A. Lauffenburger, and F. T. Serota. 1985. Use of cell affinity chromatography for separation of lymphocyte subpopulations. *Biotechnol. Bioeng.* 27:603–612.
5. Berenson, R. J., W. I. Bensinger, and D. Kalamasz. 1986. Positive selection of viable cell populations using avidin-biotin immunoadsorption. *J. Immunol. Methods.* 91:11–19.
6. Bell, G. I. 1978. Models for specific adhesion of cells to cells. *Science.* 200:618–627.
7. Bell, G. I. 1981. Estimate of the sticking probability for cells in uniform shear flow with adhesion caused by specific bonds. *Cell Biophys.* 3:289–304.
8. Hammer, D. A., and D. A. Lauffenburger. 1987. A dynamic model for receptor-mediated cell adhesion to surfaces. *Biophys. J.* 52:475–487.
9. Martin, P. J., E. R. Giblett, and J. A. Hansen. 1982. Phenotyping human leukemic T-cell lines: enzyme markers, surface antigens, and cytogenetics. *Immunogenetics.* 15:385–398.
10. Van, N. T., M. Raber, G. H. Barrows, and B. Barlogie. 1984. Estrogen receptor analysis by flow cytometry. *Science.* 224:876–879.
11. Seeger, R. C., D. D. Vo, J. Ugelstad, and C. P. Reynolds. 1986. Removal of neuroblastoma cells from bone marrow with monoclonal antibodies and magnetic immunobeads. *In* Transfusion Medicine: Recent Technological Advances. K. Murawshi and F. Peetom, editors. Alan R. Liss, Inc., New York. 285–293.
12. Pratt, B. M., D. Forn, and J. A. Madri. 1985. Endothelial cell-extracellular matrix interactions. *Ann. N. Y. Acad. Sci.* 460:274–288.
13. Albelda, S. M., M. Daise, E. N. Levine, and C. A. Buck. 1989. Identification and characterization of cell-substratum adhesion receptors on cultured human endothelial cells. *J. Clin. Invest.* 83:1992–2002.
14. McQuarrie, D. A. 1967. Stochastic approach to chemical kinetics. *In* Supplementary Review Series in Applied Probability. Volume 8. J. Gani, editor. Methuen & Co. Ltd., London. 1–68.
15. Cozens-Roberts, C., J. A. Quinn, and D. A. Lauffenburger. 1990. Receptor-mediated adhesion phenomena. Model studies with the Radial-Flow Detachment Assay. *Biophys. J.* 58:107–125.
16. McClay, D. R., G. M. Wessel, and R. B. Marchase. 1981. Intercellular recognition: quantitation of initial binding events. *Proc. Natl. Acad. Sci. USA.* 78:4975–4979.
17. Bongrand, P., and P. Golstein. 1983. Reproducible dissociation of cellular aggregates with a wide range of calibrated shear forces: application to cytolytic lymphocyte-target cell conjugates. *J. Immunol. Methods.* 58:209–224.
18. Hubbard, B. B., M. W. Glacken, J. R. Rodgers, and R. R. Rich. 1990. The role of physical forces on cytotoxic T cell-target cell conjugate stability. *J. Immunol.* 144:4129–4138.
19. Sanders, D. H., R. J. Eng, and A. F. Murph. 1985. Statistics: A Fresh Approach. McGraw-Hill, Inc., New York. 524 pp.
20. Curtis, A. S. G. 1964. The mechanism of adhesion of cells to glass. *J. Cell Biol.* 20:195–215.
21. Gingell, D., and I. Todd. 1979. Interference reflection microscopy. A quantitative theory for image interpretation and its application to cell-substratum separation measurement. *Biophys. J.* 26:507–526.
22. Gingell, D., I. Todd, and O. S. Heavens. 1982. Quantitative interference microscopy: effect of microscope aperture. *Optica Acta.* 29:901–908.
23. Press, W. H., B. P. Flannery, S. A. Teukolsky, and W. T. Vetterling. 1989. Numerical Recipes: The Art of Scientific Computing. Cambridge University Press, New York. 702 pp.
24. Vetterling, W. T., S. A. Teukolsky, W. H. Press, and B. P. Flannery. 1990. Numerical Recipes Example Book. Cambridge University Press, New York. 179 pp.
25. Ames, W. F. 1977. Numerical Methods for Partial Differential Equations. Academic Press, Inc., San Diego, CA. 365 pp.
26. Hoel, P. G., S. C. Port, and C. J. Stone. 1971. Introduction to Probability Theory. Houghton Mifflin Co., Boston. 258 pp.
27. McQuarrie, D. A. 1963. Kinetics of small systems. I. *J. Chem. Phys.* 38:433–436.
28. Dembo, M., D. C. Torney, K. Saxman, and D. A. Hammer. 1988. The reaction-limited kinetics of membrane-to-surface adhesion and detachment. *Proc. R. Soc. Lond. B.* 234:55–83.
29. Perelson, A. J., B. Goldstein, and S. Rocklin. 1980. Optimal strategies in immunology III. The IgM-IgG switch. *J. Math. Biol.* 10:209–256.
30. Hammer, D. A., and S. M. Apte. 1992. Simulation of cell rolling and adhesion on surfaces in shear flow: general results and analysis of selectin-mediated neutrophil adhesion. *Biophys. J.* 63:35–57.